JCTC Journal of Chemical Theory and Computation

Computational Studies on Polarization Effects and Selectivity in K^+ Channels

Christopher J. R. Illingworth, Simone Furini, and Carmen Domene*

Physical and Theoretical Chemistry Laboratory, Department of Chemistry, University of Oxford, Oxford OX1 3QZ, United Kingdom

Received May 26, 2010

Abstract: Umbrella sampling in combination with a polarizable QM/MM model have been used to study the role of electrostatics and polarization in the translocation and selectivity properties of two K^+ channels, KcsA and KirBac, with ions traversing the channel according to an ion−water−ion mechanism. Analysis of electrostatic interaction energies shows an increased electrostatic gradient within the KirBac channel relative to KcsA. Quantitative measurements of polarization effects induced by ions and water molecules in the channel suggest a decreased interaction with K^+ and Rb^+ close the S2 binding site. This effect cannot be explained solely by the geometry of the polarizable region, or by conformational changes in the filter, but appears to be due to the polarization of the valine residue of the TVGYG selectivity filter motif. We observe that the presence of an ion in the S2 site, and the absence of an ion at the S3 site, where there is a water molecule instead, depolarizes valine and, hence, decreases the interaction energy between that residue and the ion in S2. Our results suggest that the incorporation of polarization effects can make an observable difference to the potential experienced by an ion in the channel.

Introduction

Potassium channels have an essential role in controlling the electric potential across cell membranes, making a vital contribution to the functioning of neurons and cardiac muscle cells, among others. An important landmark in the understanding of these proteins was the first derivation by crystallography of the 3D structure of a potassium channel, namely KcsA,[1] followed by other potassium channel structures, including that of the inwardly rectifying channel KirBac1.1.[2]

These two channels share many structural features. Each channel is a tetramer, composed of identical subunits, and contains the TVGYG sequence motif characteristic of potassium channels[3] (Figure 1a). This sequence motif is called the selectivity filter, and it allows for the fast diffusion of K^+ ions, occurring at a rate approaching 10^8 ions per second,[4] while providing a very strong selectivity for K^+ over Na^+. Experimental studies measuring the conductance of the KcsA channel under symmetrical solution conditions show a more moderate preference for K^+ over Rb^+, such that the rates of diffusion can be represented as $K^+ > Rb^+ \gg Na^+$ [5]. Crystallographic studies have shown that within the selectivity filter, K^+ ions are coordinated by the backbone carboxyl groups of the protein, binding in five locations.[6] These binding sites are often denoted S0 to S4, the number increasing with distance into the intracellular region.

Two challenges in modeling potassium channels have been noted in the literature. First, the average time required for the permeation of an ion is long relative to the time scales typically employed for classical molecular dynamics (MD) simulations. This has led to the use of a range of techniques in order to obtain information about the selectivity and the ion permeation, including umbrella sampling,[7,45] steered molecular dynamics,[8] free energy perturbation,[9] or metadynamics.[10] Second, studies of K^+ and other ion channels have highlighted the potential importance of polarization effects in systems of this nature,[11] and the limitations in using common classical force fields where these effects are often neglected. One solution to this question, followed to an extent in this paper, is the use of quantum mechanical methods to model the ions and the selectivity filter.[12] For example, *ab*

* Corresponding author telephone: +44-1865285401; fax: +44 1865 275410; e-mail: carmen.domene@chem.ox.ac.uk.

10.1021/ct100276c
Published on Web 11/12/2010

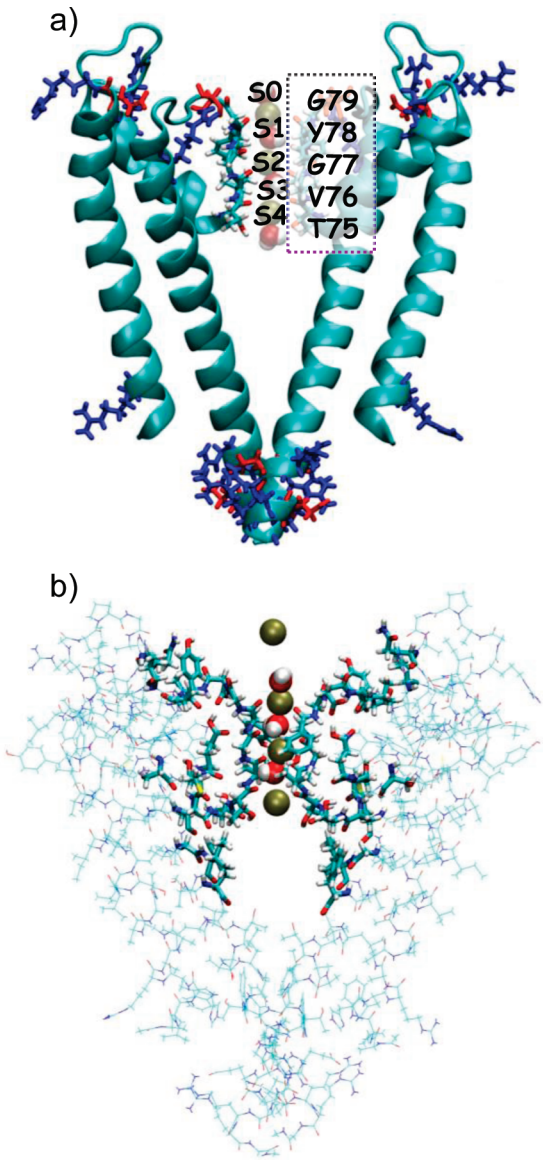

Figure 1. (a) Representation of the selectivity filter of KcsA. Just two of the four chains of the protein are shown for simplicity. The selectivity motif TVGYG is shown in licorice representation, colored by atomic type. Charged residues in the protein are shown in licorice representation, colored by charge, with positively charged residues in blue and negatively charged residues in red. The remainder of the protein is drawn in cartoon representation. The ion−water−ion−water pattern can be seen in the channel in VM representation, with water molecules and ions labeled according to binding site. (b) Representation of the model system in KcsA. Just two of the four chains of the protein are shown. Atoms in the QM region are shown in VDW representation. Atoms in the polarizable MM region are shown in licorice representation. Protein atoms in the nonpolarizable MM region are shown in line representation.

initio geometry optimizations have been used to model protein−ion interactions at the ends of the selectivity filter,[13] and the intracellular entrance of the KcsA channel.[14] Current technology allows for systems of over 400 atoms to be modeled in this way, for example, in demonstrating the role of water in the protein cavity in selectivity between K^+, Na^+, and other ions.[15] In a popular approach to studies of selectivity, *ab initio* calculations are carried out in this manner on a representative structure of either a single binding site[13,16] or another region in the channel,[14,15] containing a single K^+ or Na^+ ion. A second approach that has been taken to quantum mechanical modeling employs snapshots of the entire channel from classical molecular dynamics trajectories, using them as a basis for single-point quantum mechanics calculations. Applied to models of the selectivity filter, this has been used in conjunction with the Merz−Kollman method of assigning partial charges to highlight the shortcomings of standard classical force field methods, in that the atomic partial charges derived for residues in the selectivity filter part of KcsA differ markedly from those used in classical methods.[17] Classical MD simulations have also been used to generate starting points for integrated Quantum Mechanics/Molecular Mechanics (QM/MM) dynamics, for example, in the application of Car−Parrinello molecular dynamics to KcsA.[12,18] In this model, close to 100 atoms are included in a QM region at the center of a classically modeled protein, a few picoseconds of Car−Parrinello dynamics are obtained via a QM/MM method, and Wannier function centers are calculated to evaluate the polarization in the channel.

Quantum mechanical models offer advantages over classical models, avoiding issues of parametrization.[12] However, they require significant amounts of computational time and, so far as dynamics is concerned, do not allow for simulations of a length sufficient to model the transport of ions in K^+ channels.

A promising approach to the modeling of polarization in protein systems is found in the number of methods that have been proposed in which polarization is incorporated into a classical system, or into the classical part of a QM/MM framework.[19] An example of this approach is the Moving Domain-QM/MM method.[20] In this method, a series of ONIOM (Our own N-layered Integrated molecular Orbital + Molecular mechanics)[21] calculations are carried out, with different residues placed in the high level system in each calculation. This is applied in an iterative fashion to modify the charges in the classical low-level system, representing the effect of polarization. Applied to residues from a portion of the KcsA channel, this method gives good agreement with *ab initio* calculations in the electrostatic potential of an ion moving along the filter.

Electrostatic and geometrical properties have each been suggested as important factors in ion selectivity.[22] The hypothesis that K^+ prefers to occupy higher coordination states than Na^+, making it more suited to the 8-fold coordination state observed in K^+ channels, has been a source of debate. MD simulation of K^+ and Na^+ complexes in aqueous solution suggested K^+ to prefer an 8-fold coordination,[23] while *ab initio* studies suggested a common preferred 4-fold coordination for both K^+ and Na^+.[24] Recently, application of Car−Parrinello molecular dynamics suggested an increased preferred coordination number for K^+ compared to that of Na^+,[25] indicating that coordination number is indeed an important factor in selectivity.

A second geometrical hypothesis is the snug-fit theory, which suggests that passage through the channel of the smaller Na^+ ion requires a distortion in the filter residues,

the energetic cost of which mitigates against ion conduction.[26] Although MD simulations have shown considerable flexibility in the selectivity filter, of a magnitude greater than the difference in size between the Na^+ and K^+ ions,[10,27] isothermal titration calorimetry methods suggest that the size of the ion is indeed of importance.[28]

Electrostatic effects have also been proposed as a mechanism for selectivity.[29] In a recent work on selectivity,[30] using small models of the selectivity filter of KcsA and that of the nonselective NaK channel, the authors propose that the pore's selectivity for K^+ over Na^+ increases with an increasing hydration number of K^+ relative to that of Na^+, increasing number of K^+ or Na^+-coordinating dipoles, and decreasing magnitude of the coordinating dipoles provided by the pore.

Therefore, the conclusions emerging from all of these studies are that ion selectivity is achieved by a combination of several factors, not exclusively structural or energetic, involving both the ion and the ion-coordinating ligands, either water or protein, the dehydration penalty of the permeating cations, the electrostatic interactions, and redistribution of charge between the cation and the channel dipoles, the architecture of the ion binding site, and the pore size and flexibility.

Polarization effects have often been suggested as being of importance in K^+ channels.[11,31] However, they have not often been included in computational models of these systems. Therefore, the aim of this work is to establish the potential importance of polarization effects in selectivity and translocation.

In our model, umbrella sampling is used to generate representative sets of structures simulating the passage of Na^+, K^+, and Rb^+ through each of the channels. These sets are then used as a basis for QM/MM calculations. In contrast to methods described in the literature in which ions are displaced along a fixed selectivity filter,[17a] here fluctuations of the protein in response to different positions of the ions are allowed. Representing the ions as QM entities removes concerns which have been raised about the parametrization of ions within a classical framework.[11c] Although the QM/MM method applied here does not allow for charge transfer between the QM ions and waters, and the MM channel, it allows for calculations on the whole protein to be carried out in a feasible amount of time and has the advantage of allowing the calculation of a discrete polarization energy for an ion. In this manner, we aim to derive a comparison between the KirBac and KcsA channels and to evaluate the effect of polarization in these systems.

Materials and Methods

Model Definitions. The atomic structures of KcsA and KirBac were based on the protein data bank entries 1K4C[32] and 1P7B,[33] respectively. Only the transmembrane pore regions were included in the channel models, i.e., amino acids A23−G123 for KcsA and amino acids A40−R151 for KirBac. N termini were acetylated, and an N-methylamide group was added to the C termini. The amino acid E71 of KcsA was modeled in the protonated state,[34] to form a diacid hydrogen bond with D80. The analogous residue in KirBac (E106) was also modeled in the protonated state. Default ionization states were used for the remaining amino acids. Four water molecules were placed at the back of the selectivity filter, in agreement with crystallographic data and previous MD simulations. The channels were embedded in a pre-equilibrated lipid bilayer of 256 1-palmitoyl,2-oleoyl-sn-glycero-3-phosphocholine (POPC) molecules. The channel axis was aligned to the bilayer normal, and the extracellular aromatic belt (amino acids Y45 in KcsA and amino acids Y82 in KirBac) was aligned to the bilayer surface. Lipid molecules closer than 1.0 Å to protein atoms were removed. The atomic systems were solvated using the *Solvate* plug-in of VMD,[35] and then water molecules within 1.2 Å of protein and lipid atoms were removed. Ions corresponding to a concentration of 150 mM of KCl, NaCl, or RbCl were added to neutralize the systems. For convenience, in comparison, the residues of the KirBac structure were renumbered to align the sequence with that of KcsA, such that the residues in the selectivity filter motif TVGYG had residue numbers 75−79. This convention is maintained throughout the remaining sections of this paper.

Molecular Dynamics Simulations. The KcsA and KirBac system models were validated by MD simulations. The same protocol was used for all of the models. Harmonic restraints with a force constant of 20 kcal mol^{-1} $Å^{-2}$ were applied to the protein backbone atoms in the first 500 ps. Then, 20 ns of unrestrained dynamics were performed. The CHARMM27 force field was used for lipids and with CMAP correction[36] for proteins, together with TIP3P model for water molecules.[37] Parameters for ions inside the selectivity filter were selected according to ref 11c, while default CHARMM parameters were used for ions in bulk solution. The particle mesh Ewald algorithm was used to treat the electrostatic interactions.[38] van der Waals forces were smoothly switched off at 10−12 Å. Bonds with hydrogen atoms were restrained by the SETTLE algorithm,[39] in order to use a 2 fs time step. The multi-time-step algorithm r-RESPA[40] was used to integrate the equation of motion. Nonbonded short-range forces were computed every time step, while electrostatic forces were updated every two time steps. MD simulations were performed in the NPT ensemble. Pressure was kept at 1 atm by the Nose−Hoover Langevin piston method,[41] with a damping time constant of 100 fs and a period of 200 fs. The temperature was kept at 300 K by coupling to a Langevin thermostat, with a damping coefficient of 5 ps^{-1}. Calculations were performed using version 2.6 of NAMD.[42] A common assumption dating back to early structural work,[43] adopted in many computational studies,[7,22a,44] is that ions traverse the channel in an ion−water−ion−water fashion. While the potential existence of other permeation pathways has been suggested elsewhere,[45] the ion−water−ion−water pattern was here chosen as the basis for simulation.

Umbrella Sampling Simulations. To obtain representative structures of the selectivity filter with ions at all positions along it, umbrella sampling simulations were carried out. The four ions involved in the conduction process were named I1 (outermost ion, extracellular side) to I4 (innermost ion, intracellular side). Three independent biasing potentials were

applied in order to control the positions along the channel axis. The center of the biasing potential acting on I4 moved from the intracellular cavity to the binding site S4, while the biasing potential acting on I1 moved from the binding site S0 to the extracellular milieu. The position along the axis of I2 and I3 was controlled by a harmonic potential acting on the center of mass of the pair, with the center of the biasing potential acting moving from a situation with ions at the binding site S4 and S2 to a situation with ions at binding sites S2 and S0. Harmonic potentials were updated in 0.5 Å steps. The force constant of the harmonic potentials was set to 20 kcal mol^{-1} $Å^{-2}$. Over 400 windows were run of 120 ps each, representing a total of 48 ns of simulation time to achieve convergence. The first 20 ps of each window were discarded as an equilibration period.

For the structures including Na^+, four sets of umbrella sampling simulations were run, with the Na^+ ion taking the place of one of the K^+ ions in the filter, respectively I1−I4 in the four sets. Thus, a total of 12 sets of umbrella sampling simulations were run, representing KirBac and KcsA with four K^+ ions, with four Rb^+, and with the various orderings of three K^+ and one Na^+ ion.

The last frame of each umbrella sampling calculation was used as an input to a QM/MM calculation in which induced charges were used to model polarization in the filter region. In this way, a comprehensive picture of the passage of ions through each of the two channels has been generated.

QM/MM Calculations. Modeling of electrostatics and, more specifically, polarization in the channel was carried out using a variant of an induced charge method,[46] adapted for modeling larger (more than 1000 atom) systems. Here, the QM region was defined as the four ions in the channel, in addition to the three water molecules closest to the filter, the waters being identified according to the minimum atom−atom distance between a water molecule and either of the middle two ions in the filter. In a previous application of the induced charge model, an enzyme−substrate system was defined in two regions, with a QM ligand surrounded by a few chosen residues of the protein represented as polarizable MM entities.[47] Here, however, the entirety of the protein structure was included, with a polarizable MM region set within a fixed-charge MM representation of the protein. Polarization effects are short-range in nature, and calculations on a charged ligand in explicit aqueous solvent[47] showed more than 75% of the polarization energy being captured by a 5 Å cutoff. Here, the cutoff was defined such that all residues with at least one atom within 9 Å of one of the middle two filter ions in at least one of the structures generated by the umbrella sampling was included in the polarizable MM region. An example of the model system is shown in Figure 1b. More details of the residues included in each case are contained within the Supporting Information. Initial charges for the MM region were taken from the CHARMM force field, as used in the umbrella sampling calculations.

Two simplifications of the induced charge model, appropriate to the study of a large protein system, were made. In small molecule systems, incorporation of polarization due to the interaction between classical parts of the system led to QM−MM interaction energies closer to those in which the MM system was represented by QM-derived charges. Here, in order to isolate polarization effects caused by the movement of ions, and in common with earlier applications of the method to protein−ligand systems,[48] this classical−classical term was omitted. Second, whereas in earlier work four or five iterations of the induced charge method were applied, the vast majority of the change in charges is captured by the first iteration, and as such, only a single iteration was applied here.

Following the induced charge model, polarization was modeled using a series of QM/MM calculations. First, a single-point calculation was carried out on the QM atoms, described above, in the presence of the protein, modeled as a set of point charges without polarization. Second, polarization was incorporated into the charges of atoms in the polarizable MM region. The electrostatic field of the QM region of the system, calculated in the presence of the MM charges using Gaussian 03,[49] was represented as a set of atom-centered multipole series, generated using the GDMA software package.[50] These were used to calculate induced multipole series on the polarizable MM atomic centers, which were then converted into modified point charges using the mulfit software package.[51] Under this process, the overall charge on each molecule within the MM system is conserved. Finally, another single-point calculation was carried out on the QM atoms in the presence of the protein, this time with polarization incorporated into the point charges. Comparing the result of this calculation with the result of the original single-point calculation gave a measure of the polarization energy. In this manner, two key values were calculated, the electrostatic interaction energy between a QM water or ion and the unpolarized channel and the polarization energy, equal to the change in the interaction energy with the addition of polarization to the polarizable region of the channel.

All QM calculations were carried out at the HF/LANL2DZ level, and some representative sets were repeated at the B3LYP/LANL2DZ and MP2/LANL2DZ levels of theory for KcsA for comparison. The LANL2DZ basis set was chosen as being roughly equivalent in quality to the 6-31G* basis set, while having been parametrized for Na^+, K^+, and Rb^+.

Ion Position Definitions. In order to compare energies from different snapshots, it was necessary to obtain a definitive measure of the position of the ions in the channel. Use of a straightforward z coordinate is potentially misleading, due to changes in the internal structure of the channel with changes of ion position, even following alignment of the residues in this region. Therefore, an alternative coordinate, referred to as the relative channel coordinate (RCC), was defined, expressing the ion position in relation to the protein binding sites S0 to S4. Details are presented in the Supporting Information.

Theoretical Basis. For each of the structures on which calculations were performed, if the set of QM atoms is labeled A, then the electrostatic interaction energy of the atoms in A with the channel, $E_{es}(A)$ was calculated as the change in the energy of the QM atoms resulting from the interaction with the unpolarized channel:

$$E_{es}(A) = E_{QMMM1}(A) - E_{QM}(A) - E_{pc1} \quad (1)$$

where $E_{QMMM1}(A)$ is the total energy of the initial QM/MM system, $E_{QM}(A)$ is the energy of the QM atoms without the surrounding MM atoms, and E_{pc1} is the self-energy of the initial point charges in the MM region. The total polarization energy $E_{pol}(A)$ was calculated as the difference between the energies of interaction, calculated as above, for the polarized and unpolarized channel:

$$E_{pol}(A) = [E_{QMMM2}(A) - E_{QM}(A) - E_{pc2}] - E_{es}(A) \quad (2)$$

where $E_{QMMM2}(A)$ is the total energy of the polarized QM/MM system and E_{pc2} is the self-energy of the polarized point charges in the MM region. That is, $E_{pol}(A)$ is the difference in the energy of interaction made by the inclusion of polarization into the MM region. Note that point charges of MM atoms outside of the polarizable region were kept constant.

In order to understand the behavior of ions and water molecules passing through the channel, it was necessary to calculate energies of interaction for individual molecules in the QM region. The interaction energy of a molecule was calculated by performing QM/MM calculations on a system in which that molecule was omitted. For any molecule m, the electrostatic interaction energy $E_{es}(m)$ of that molecule with the rest of the system was defined as

$$E_{es}(m) = E_{es}(A) - E_{es}(A_m) \quad (3)$$

where A_m is the set of QM atoms excluding molecule m and $E_{es}(A_m)$ is calculated according to eq 1.

Applied to an ion, this energy is equal to the sum of the electrostatic energies of interaction between the ion and the other ions and QM waters, and that between the ion and the channel itself. In order to derive the interaction energy of an ion or water molecule with the channel excluding ion−ion effects, the QM−QM interaction energy $E_{QM}(m)$ was defined as the *in vacuo* interaction of a molecule in the QM region with the rest of the QM region and was subtracted from the total interaction energy $E_{es}(m)$ (defined in eq 3). The interaction energy of a molecule m with the channel is thus

$$E_{channel}(m) = E_{es}(m) - E_{QM}(m) \quad (4)$$

Similarly, the polarization energy between the molecule m with the channel, $E_{pol}(m)$, was defined as

$$E_{pol}(m) = E_{pol}(A) - E_{pol}(A_m) \quad (5)$$

where $E_{pol}(A_m)$ was calculated according to eq 2.

By the separation of individual energies of interaction outlined above, and the consideration of multiple structures with multiple ion and water positions relative to the channel, it is possible to obtain an interaction energy profile describing the passage of ions through the channel. Energy values for ions and waters were averaged over bins of RCC length 0.1 in order to calculate this. It is important to note that this interaction energy profile describes the energy of interaction between the ions and the channel. Effects such as desolvation are omitted in order to isolate terms arising from the interaction of the ions and the channel. These interaction energies should not be confused with free energy differences.

Calculations for the KcsA channel with K^+ ions were repeated using the B3LYP/LANL2DZ and MP2/LANL2DZ levels of theory, generating electrostatic interaction and polarization energy profiles for ions moving through the channel. The electrostatic interaction in each case was virtually identical to that found at the HF level of theory. The overall shape of the polarization energy profiles was preserved.

By means of similar calculations, it was possible to carry out residue-by-residue decompositions of the electrostatic and polarization energies. The electrostatic interaction between a QM molecule and a residue within the protein was calculated as described in eq 3, with the MM region containing only the residue in question. This method was used to measure the contributions of different residues to selectivity in the S2 site, the S2 binding site exhibiting the maximal selectivity between Na^+ and K^+ ions.[16a] The polarization energy of interaction between a QM molecule and a residue within the protein was similarly calculated as described in eq 5, with the MM region only containing the residue in question. For polarization calculations, the polarized charges for the residue were taken from the polarized charges generated for the entire QM/MM system. Note that due to the symmetry of the system, when a single residue is considered, this in fact corresponds to four identical amino acids, one from each of the identical protein chains.

Modeling polarization in this way is complicated by the fact that the polarizable region is finite and undergoes small geometrical changes between snapshots, and by the fact that ions move relative to this region. As the polarization energy is dependent on the region over which it is measured, this leads to an inherent variation in the calculated polarization energy as an ion moves through the polarizable region. In order to model the effect of these relative changes in geometry on the polarization energy, a geometrical factor was calculated, giving an indication of the expected polarization energy at each ion position relative to the channel. Modeling the ion, *i*, as a unit charge and placing unit dipoles at each of the atoms *j* in the polarizable region gave the sum of charge−dipole interactions:

$$P_G(i) = \sum_{j=1}^{N} \frac{1}{r_{ij}^2} \quad (6)$$

where r_{ij} is the distance between *i* and *j*. This factor gave a reference against which calculated polarization energies could be compared.

Results

In order to analyze the QM/MM data, results for single ions were grouped by RCC in bins of width 0.1, equal to a tenth of the distance between binding sites. Average values of the electrostatic interactions were calculated for each of the RCC bins. In addition to a combined energy, representing the interaction of an ion with the remainder of the system, the interaction energies with the QM system, and with the protein, were calculated separately. Figure 2 shows mean

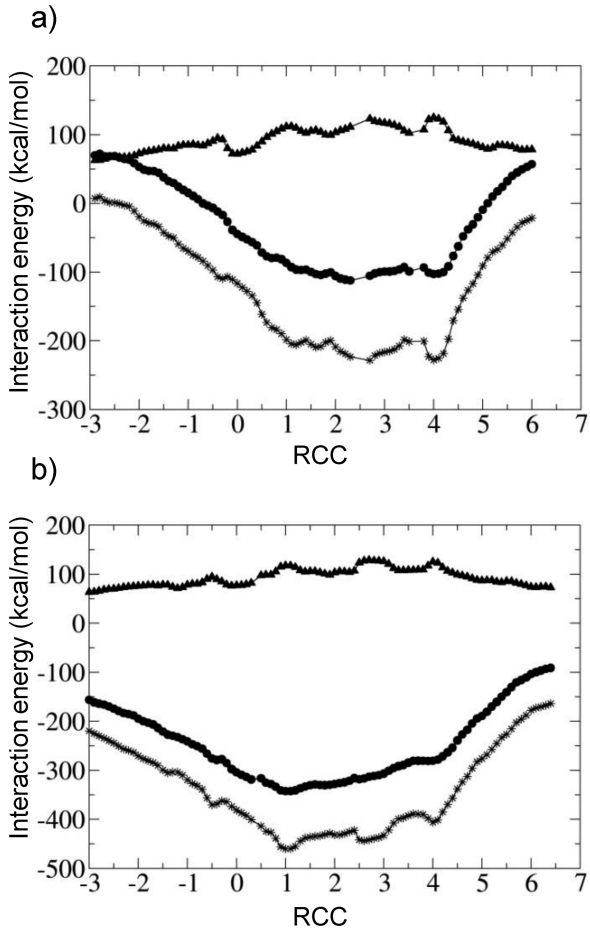

Figure 2. Averaged electrostatic interaction energies of K^+ ions moving through the selectivity filters of (a) KcsA and (b) KirBac. For each system, the total interaction energy (circles), the QM−QM interaction energy (triangles), and the ion−protein interaction energy (stars) are plotted.

electrostatic interaction energies for K^+ ions passing through the two different channels. Equivalent data for Na^+ and Rb^+ are given in Supporting Information Figure S1. Each point in the figure represents a collection of structures. Note that the energies, representing the interaction of the ion with the channel, exclude factors such as desolvation and should not be confused with free energy differences. While the position of the ion in question is denoted by the RCC, plotted on the horizontal axis, the remaining three ions can occupy a range of positions, leading to variations in the energy that are in general removed by averaging over the snapshots in each bin.

Absolute electrostatic interaction energies, by contrast to free energy differences, are large, on the order of hundreds of kilocalories per mole.[52] Examination of the these energies revealed that Na^+ ions have a stronger electrostatic interaction with the channel than do K^+ or Rb^+. In order to compare the behaviors of the different ions, mean electrostatic interaction energies were calculated for ions for which the RCC was between 1 and 4 (i.e., in the filter region). The differences between these energies were then corrected, subtracting the differences between the experimentally observed desolvation energies of the ions.[53] In KcsA, the corrected mean interaction with K^+ was 2.1 kcal/mol greater than that of Rb^+, and 6.5 kcal/mol greater than that for Na^+, while for KirBac, the K^+ interaction was 2.0 kcal/mol greater than that for Rb^+, and 12.8 kcal/mol greater than that for Na^+. Accurate characterization of ion selectivity requires the balancing of many subtle factors and is not easy with either classical or quantum mechanical approaches. In this case, a greater level of sampling at the QM/MM level would inevitably bring a greater degree of accuracy, though the ordering of energies found here ($K^+ > Rb^+ > Na^+$) was consistent with experimental measurements.[5]

Table 1. Mean Electrostatic Interaction Energies for Ions in Binding Sites S1 to S4 with the Amino Acids of the TVGYG Motif and Another Residue in KcsA and KirBac[a]

residue			mean interaction energy (kcal/mol)	
KcsA	KirBac	binding site	KcsA	KirBac
Thr75	Thr75	S1	−2.6 ± 1.4	−4.6 ± 1.2
Thr75	Thr75	S2	−15.6 ± 4.9	−15.8 ± 3.5
Thr75	Thr75	**S3**	**−58.9 ± 6.5**	**−59.3 ± 4.5**
Thr75	Thr75	**S4**	**−109.5 ± 8.0**	**−101.9 ± 10.9**
Val76	Val76	S1	−16.3 ± 5.1	−22.3 ± 1.4
Val76	Val76	**S2**	**−43.0 ± 7.3**	**−55.8 ± 8.0**
Val76	Val76	**S3**	**−36.9 ± 7.9**	**−47.0 ± 5.3**
Val76	Val76	S4	−10.8 ± 2.6	−14.2 ± 2.0
Gly77	Gly77	**S1**	**−62.7 ± 3.6**	**−58.1 ± 4.8**
Gly77	Gly77	**S2**	**−64.9 ± 4.6**	**−59.6 ± 3.7**
Gly77	Gly77	S3	−23.3 ± 3.9	−19.1 ± 2.3
Gly77	Gly77	S4	−6.5 ± 1.1	−7.2 ± 1.3
Tyr78	Tyr78	**S1**	**−27.0 ± 7.2**	**−45.4 ± 3.9**
Tyr78	Tyr78	S2	−4.9 ± 1.9	−8.5 ± 2.9
Tyr78	Tyr78	S3	−2.6 ± 1.2	−5.1 ± 1.2
Tyr78	Tyr78	S4	0.5 ± 0.7	−0.9 ± 0.9
Gly79	Gly79	S1	−0.4 ± 1.4	−6.9 ± 2.6
Gly79	Gly79	S2	4.4 ± 1.1	2.5 ± 2.2
Gly79	Gly79	S3	3.9 ± 0.6	2.3 ± 0.8
Gly79	Gly79	S4	3.3 ± 0.2	2.7 ± 0.7
Arg52	Ala52	S1	49.6 ± 0.7	0.2 ± 0.1
Arg52	Ala52	S2	48.1 ± 0.6	0.1 ± 0.2
Arg52	Ala52	S3	46.2 ± 0.6	−0.2 ± 0.1
Arg52	Ala52	S4	44.0 ± 0.5	−0.3 ± 0.1

[a] Each energy value is calculated from a representative set of structures; the standard deviation gives a measure of the variability of the energy in each case. Interaction energies making the largest contributions to the electrostatic interaction with ions in different sites are highlighted in bold.

Sets of structures of KcsA and KirBac containing ions with an RCC equal to 1.0, 2.0, 3.0, or 4.0 were selected, and average residue-by-residue electrostatic interaction energies were calculated for ions in each system at each of these points. Some representative results for these interactions are shown in Table 1. Unsurprisingly, for both protein systems, the largest residue differences between ion positions occurred for residues of the selectivity filter, which comprise the ionic binding sites. For each system, differences between the residue electrostatic interaction energies with ions in S1 and in S4 were summed across all residues, giving an approximation to the overall difference in binding energies between ions in S1 and ions in S4. As can be seen in Figure 1, for structures analyzed here, the interaction energy between the KcsA channel and ions at S4 is slightly stronger than that at S1, while the interaction energy between KirBac and ions at S4 is significantly weaker than that at S1. Residue-by-residue comparison of the sequences, carried out on the basis of the alignment in ref 33, suggests that a number of factors contribute to this effect. First, the electrostatic interaction between the ion in the S1 site and the residues

Table 2. Breakdown of Electrostatic Interaction Energies between Na^+, K^+, and Rb^+ Ions in the S2 Site of KcsA and KirBac[a]

	KcsA			KirBac		
	Na^+	K^+	Rb^+	Na^+	K^+	Rb^+
sum of residue interactions for all residues (kcal/mol)	−113.7	−104.2	−100.7	−335.1	−333.2	−319.2
relative binding energy of ion with all residues, corrected for desolvation (kcal/mol)	+7.2	0.0	−1.3	+14.8	0.0	+9.3
sum of residue interactions for residues TVGYG (kcal/mol)	−135.8	−124.2	−120.1	−139.5	−137.2	−125.8
relative binding energy of ion with residues TVGYG, corrected for desolvation (kcal/mol)	+5.1	0.0	−0.7	+14.5	0.0	+6.7

[a] Relative energies are calculated by subtracting experimental values for desolvation from the interaction energies and are given relative to that for K^+.

Y78 and G79 is significantly stronger in KirBac than in KcsA (as mentioned earlier, for convenience, in comparison, the residues of the KirBac structure were renumbered to align the sequence with that of KcsA, such that the residues in the selectivity filter motif TVGYG had residue numbers 75−79). Second, KcsA and KirBac have a different distribution of charged and uncharged residues. In both proteins, charged residues are clustered away from the center of the cell membrane. However, in the extracellular region, KcsA contains the positively charged residues R52, R64, and R89, in addition to the negatively charged residues E51 and D80. In the intracellular region, KcsA contains the positively charged R117, R121, R122, and R27 and the negatively charged residues E118 and E120 (see Figure 1a). No charged residues occur toward the center of the cell membrane. Therefore, in KcsA, ions being transported out of the cell move from a region of the protein with an overall charge of +8 to a region with an overall charge of +4. In KirBac, however, the distribution is different. The extracellular region contains the negatively charged residues D51 and D80, with E95 slightly buried into the membrane region and E71 in a neutral protonation state, while the intracellular region contains the positively charged residues R14, K22, R113, and R116 and the negatively charged D15. Thus, ions being transported out of the cell move from a region of the protein with an overall charge of +12 to a region with an overall charge of −12. This creates a differing energy gradient which can be observed in the residue differences. As illustrated in Table 1, the movement of the positively charged ion away from, for instance, R52 in KcsA contributes to the favorability of S4 over S1, an effect that is not present in the equivalent neutral residue in KirBac. Electrostatic interaction energies with ions in the S2 and S3 positions are intermediate to those for S1 and S4, corresponding to the positions of the ions relative to these charged residues. While the observed difference in the interaction energies with charged residues would be reduced by the internal dielectric constant of the protein, the sum of the long-range interactions with charged residues is non-negligible.

Residue-by-residue interactions were also calculated for structures of KcsA and KirBac containing either a Na^+ or Rb^+ ion with RCC equal to 2.0. Results are shown in Table 2. Taking the sum of all of the residue interactions in each case, Na^+ bound more strongly than K^+. A larger difference in binding energy was also observed for Rb^+ in KirBac, although in KcsA, Rb^+ bound more strongly in the S2 site than did K^+. In each case, the residues in the TVGYG filter motif made a substantial contribution to the relative binding energies of the ions, accounting for between 50 and 98% of the calculated energy difference.

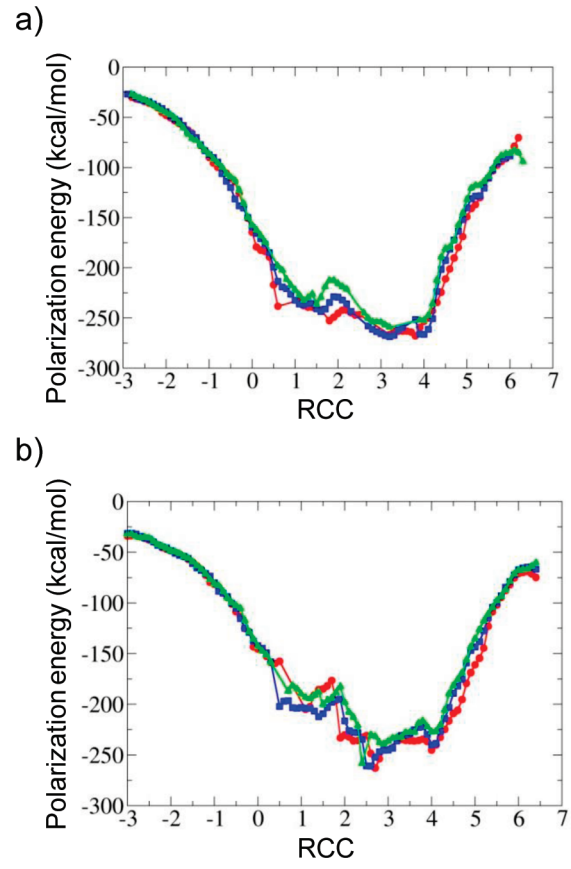

Figure 3. Averaged polarization energies of K^+ ions (blue squares), Na^+ ions (red circles), and Rb^+ ions (green triangles) moving through the selectivity filter of (a) KcsA and (b) KirBac.

Average values of the polarization energy were calculated for each bin in a similar manner to the electrostatic energies (Figure 3). As already noted, the polarization energy is dependent on the position of the ion relative to the polarizable region of the protein, and therefore, it is more difficult to compare energies at different ion positions. However, this does not affect the comparison of different ions at identical positions in the filter, and in this measure, a pattern similar to that in the electrostatic energies was observed.

Averaged polarization energies were calculated for ions in the filters of each KcsA and KirBac. No consistent pattern

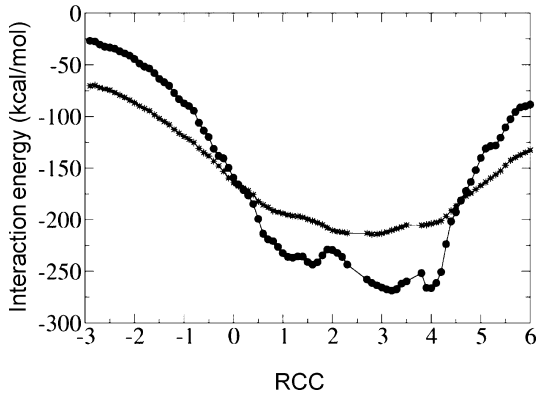

Figure 4. Measured (circles) and expected (stars) polarization energies of K^+ ions moving through the KcsA selectivity filter. Linear scaling has been applied to the latter measure in order to give identical mean values, thereby aiding comparison of the shapes of the graphs.

was observed for the relative polarizations of K^+ and Na^+. In KcsA, Na^+ had slightly greater polarization energy than K^+, while in KirBac the polarization of Na^+ was lower than that of K^+. In each case, the polarization energy of K^+ tended to be stronger than that of Rb^+.

An interesting feature of the polarization energy is the presence of a peak representing low polarization energy at a relative channel coordinate of around 2, seen for both K^+ and Rb^+ ions in both KcsA and KirBac. A similar feature is also observed for Na^+ ions, albeit less pronounced and at a relative channel coordinate slightly greater than 2 in KcsA, and slightly less than 2 in KirBac. Calculation of expected polarization energies suggested that this feature is not simply an artifact of the geometry of the polarizable region. A comparison of the expected polarization energy with the measured averaged polarization energies for K^+ in KcsA is shown in Figure 4. A constant term has been added to the former measure in order to give identical mean values, thereby aiding comparison of the shapes of the graphs.

The expected values here demonstrate that the movement of the ions through the polarizable region has a significant effect on the measured polarization energy. Toward the edges of the polarizable region, the expected polarization decreases due to the decrease in polarizable volume in the immediate vicinity of the ion. This contributes in part to the increase in the measured polarization energy in the filter region relative to that in the cavity and external regions. However, the decreased polarization measured at S2 cannot be explained by the movement of the ion relative to the polarizable region.

An additional factor considered as a possible source of lowered polarization energy in the S2 site was the presence of changes in the conformation of the backbone of the channel residues. In some of the structures analyzed, flips in one of the Val76 residues were observed, such that the carbonyl group of the residue pointed away from the center of the channel. Flipping of carbonyl ligands is an ordinary observation in K^+ channels, as described in various computational studies for different K^+ channels.[54] Average interaction and polarization energies were calculated as above for a set of structures edited so that these flips did not occur, and for a randomly edited set of structures, where an identical number of randomly chosen structures were removed (results shown in Supporting Information Figure S2). A difference between the sets was observed close to S2, with an increase in both the electrostatic interaction energy and the polarization energy when the flips were removed, likely due to the interaction with the additional carbonyl group present when no flip occurs. Despite this increase, however, the overall character of the polarization energy profile was unaffected.

A residue-by-residue breakdown of polarization energy was carried out for structures from the umbrella sampling calculations for KcsA and KirBac with four K^+ ions. Residue-by-residue polarization energies were calculated for structures containing ions with an RCC of 1.0, 1.6, 1.7, 1.8, 1.9, 2.0, 3.0, or 4.0, thereby providing detail of the polarization interaction at each binding site. In each case, the vast majority of the polarization energy was captured by the interaction of ions with the residues in the TVGYG selectivity motif, with other residues in the polarizable region contributing 10% or less of the total polarization energy. Table 3 shows mean polarization energies for residues in

Table 3. Residue-by-Residue Breakdown of Single Ion Polarization Energies for K^+ Ions at Different Locations in the Selectivity Filter (TVGYG Motif) of KcsA and KirBac[a]

	mean polarization energy (kcal/mol), ion and RCC									
	K^+	K^+	K^+	K^+	K^+	K^+	K^+	K^+	Na^+	Rb^+
residue	1.0	1.6	1.7	1.8	1.9	2.0	3.0	4.0	2.0	2.0
					KcsA					
T75	−23.6	−34.4	−33.8	−48.2	−62.3	−62.5	−96.2	−197.5	−45.9	−61.2
V76	−53.1	−91.6	−89.8	−81.2	−68.6	−75.9	−122.6	−45.0	−84.3	−69.4
G77	−63.7	−61.2	−65.3	−58.9	−59.6	−60.3	−19.3	−6.8	−82.7	−51.8
Y78	−38.5	−37.9	−33.6	−29.3	−15.3	−17.8	−13.5	0.1	−22.7	−18.0
G79	−56.2	−24.1	−18.4	−17.1	−16.8	−17.7	−15.6	−8.1	2.2	−12.7
total	−240.5	−252.6	−248.3	−239.6	−231.8	−242.2	−277.3	−280.5	−266.3	−222.2
					KirBac					
T75	−26.4	−34.9	−37.9	−42.6	−52.9	−51.3	−94.4	−171.8	−33.2	−56.3
V76	−73.9	−98.8	−98.9	−105.9	−97.4	−101.2	−146.9	−72.1	−87.7	−86.5
G77	−58.9	−68.8	−66.2	−54.8	−52.3	−65.5	−15.9	−9.2	−79.0	−50.6
Y78	−93.5	−60.0	−45.9	−40.1	−32.2	−17.9	−21.1	0.4	−51.9	−25.9
G79	1.2	1.9	5.3	3.7	7.7	−4.5	−0.4	−1.0	0.5	−1.3
Total	−244.8	−252.9	−239.7	−237.9	−226.2	−238.2	−276.2	−254.9	−245.9	−218.9

[a] Values for Na^+ and Rb^+ are given for the center of the S2 binding site, this site exhibiting the maximal selectivity between ions.

the selectivity filter, in structures containing ions with specific relative channel coordinates.

Certain patterns can be observed in the residue-by-residue polarization energy data. For example, in KcsA, the polarization energy due to the residue T75 steadily increases in magnitude as the RCC of a K^+ ion increases from 1.0 to 4.0, this effect being easily explained by the increasing proximity of the ion to this residue as the RCC increases. Simultaneously, the components of the polarization energy due to the interactions with Y78 and G79 exhibit a constant decrease in magnitude with increasing RCC, as the distance between the ion and these residues increases. The polarization energy due to the interactions with V76 and G77 are more complex. As might be expected, the interaction with V76 achieves its greatest value when an ion has a RCC of 3.0, in which case the carboxyl group of the residue is directly involved in binding the ion. However, when the RCC of the ion is increased from 1.6 to 2.0, moving toward this residue, there is a decrease in the magnitude of the polarization interaction. Figure 5 shows the mean changes in charge with polarization in the T75 and V76 residues for structures of KcsA containing a K^+ ion with an RCC of either 1.6 or 2.0 (details for other residues given in Supporting Information Figures S4 and S5). Changes in charge have been averaged over the four copies, one per chain, of each residue. In general, the magnitude of the changes in the atom charges reflects
the magnitude of the polarization energies recorded in Table 3. For example, the polarization energy captured by the T75 residue increases in magnitude as the RCC of the ion increases from 1.6 to 2.0. Corresponding with this movement, the change in the charge of the α carbon atom of this residue also increases in magnitude, from −0.15 to −0.29. Examination of the charges in the V76 residue shows that at each ion position, the polarization increases the magnitude of the negative charge on the carbonyl oxygen, as would be expected for an interaction with a set of positively charged ions. However, as the ion moves closer to this carbonyl group, its RCC increasing from 1.6 to 2.0, the amount of polarization decreases, a surprising result. Some explanation for this can be seen in Figure 6, which shows the distribution of the RCC of the ion adjacent to that with an RCC between 1.6 and 2.0, moving into the cell. For the purposes of the figure, the RCC of the second ion is rounded to the nearest integer value. When the first ion is located further into the channel, its RCC increasing from 1.6 to 2.0, the location of this next ion also changes so that the RCC of this second ion is 4 or above in all of the observed structures. Hence, the increase in the RCC of an ion from 1.6 to 2.0 is associated with a second ion leaving the S3 binding site, away from the carbonyl oxygen of the V76 residue. This decreases the polarization of this residue, lowering the energy of polarization between V76 and the ion further up the channel. Hence, binding of an ion in the S2 binding site is affected by polarization effects that result from the interaction with other ions further into the channel. Repeat calculations performed for a single Na^+, K^+, or Rb^+ ion moving through KcsA or KirBac, for which the other binding sites

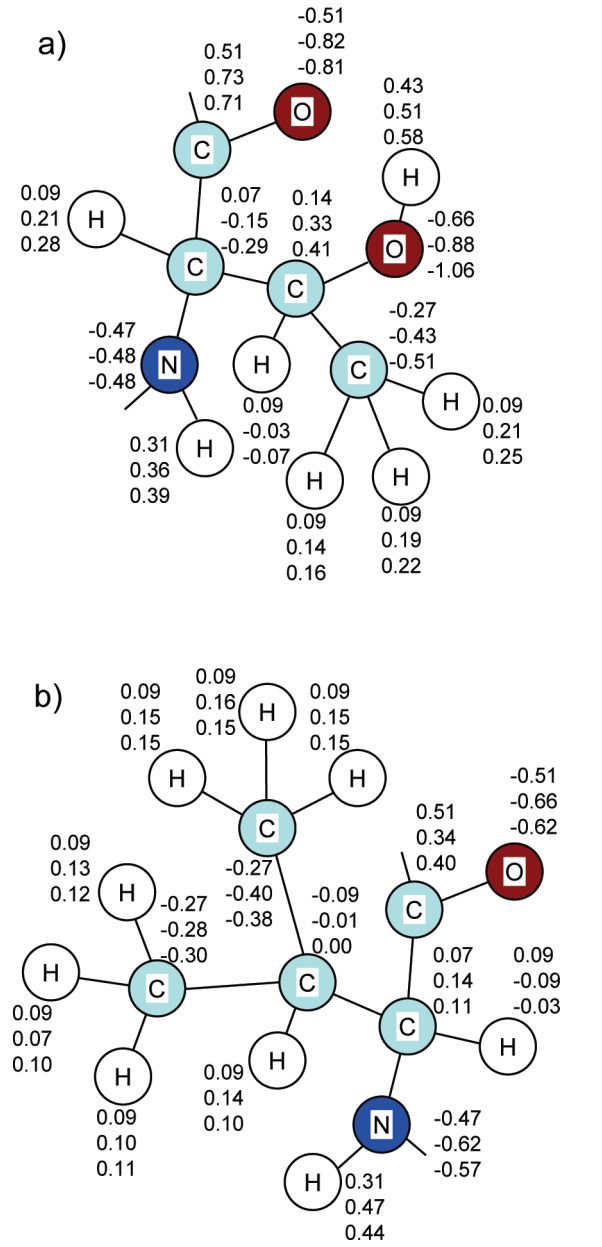

Figure 5. Mean atomic charges in the (a) T75 and (b) V76 residues of KcsA before and after polarization of the channel in structures. Charges are given for the unpolarized system (top), and for structures with K^+ ions at RCC values of 1.6 (middle number) and 2.0 (bottom number). Changes are averaged over the atoms in the four V76 residues in each case.

were occupied by water molecules, did not show the same effect at S2.

In KirBac, patterns broadly similar to those seen in KcsA can be observed, with differences in the polarization interactions of V76 and G77 leading to a drop in the magnitude of polarization at S2 as the RCC of a K^+ ion increases from 1.6 to 2.0. Analysis of changes in charges again showed a decrease in the magnitude of polarization of the carbonyl oxygen of V76 occurring as a result of this movement. As with KcsA, this can be associated with interactions taking place further down the channel. A difference between KcsA and KirBac occurs in residues Y78 and G79. In KcsA, the

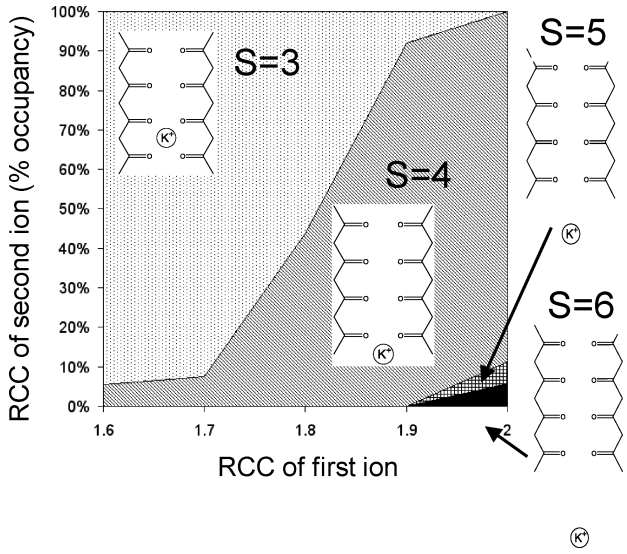

Figure 6. Distribution of the RCC of the next ion into the KcsA channel, for structures containing an ion with an RCC between 1.6 and 2.0. The RCC of the first ion is given on the horizontal axis, while the vertical axis shows the distribution of the RCC of the second ion. The RCC of the second ion is rounded to the nearest integer and takes values of 3 (dotted shading), 4 (diagonal shading), 5 (hashed shading), or 6 (solid shading). Inset figures indicate the position of the second ion. As the RCC of the first ion increases from 1.6 to 2.0, the second ion leaves the S3 site and moves into S4 or a location further into the channel.

polarization of these residues is split between the two residues, while in KirBac, it is concentrated in changes in the charges of the tyrosine residue.

Electrostatic interaction and polarization energies calculated for water molecules in the channels were much smaller in magnitude than those calculated for the ions.

Discussion and Conclusions

By means of a series of umbrella sampling calculations, we have obtained a complete set of structures of Na^+, K^+, and Rb^+ ions passing through the KcsA and KirBac selectivity filters. The umbrella sampling method provides a representative set of sample structures for the QM/MM calculations with a number of advantageous properties. First, ions can be located in a range of different places within the filter region, not being constrained to the positions of lowest energy. Second, the freedom of the ions to move relative to each other allows for the sampling of a range of different ion configurations given that one ion is in a specific point in the channel. Third, throughout the simulations, the protein is unfixed, allowing for the channel to respond to the movements of the ions.

Whereas, in some previous work, QM calculations have been carried out on some averaged channel structures[17a] or by running dynamics calculations from a small number of starting structures,[12] we have extended the induced charge method of polarization to carry out polarizable QM/MM calculations on a complete representative set of classically generated structures. The use of quantum mechanical methods has the advantage of avoiding questions of parametrization of ions, while the incorporation of polarization into a classical force field has the advantage of allowing for the calculation of electrostatics and polarization in a large number of structures in a reasonable amount of time. Although our QM/MM methodology does not incorporate charge transfer, potentially leading to a slight inflation in the interaction energies with the selectivity filter, we do not anticipate that this omission would alter the fundamental nature of the results obtained.

Energetic calculations carried out in a QM/MM framework showed mean binding energies consistent with those observed experimentally, with a slight preference in binding for K^+ over Rb^+, and a more significant difference between K^+ and Na^+. Comparison of the electrostatic interaction energies for KirBac and KcsA highlight the existence of an electrostatic gradient in the KirBac filter not present in KcsA, with a significantly higher energy for an ion in the S4 binding site than in the S1 binding site. Two factors are presented in explanation of this: first, an energy contribution resulting from the residues of the TVGYG selectivity motif and, second, a distribution of charged residues in the intra- and extra-cellular regions of KirBac disfavoring to an extent the passage of ions from S1 to S4. The second of these carries the implication that residues relatively far from the selectivity filter can affect the electrostatic energies of K^+ and Rb^+ ions moving through it. Changes in the electrostatic energy may modify the conductance properties of the channels. Thus, the conductance variability observed in the K^+ channel family may partially be explained by an electrostatic effect of nonconserved residues surrounding the selectivity filter.

Calculations of the polarization energy of each ion were made using a QM/MM induced charge method applied to a classical representation of the protein. Modeled in this way, polarization was observed to be a short-range effect, with 90% or more of the polarization energy caused by the ions being captured by the residues in the TVGYG filter motif. As noted in the electrostatic interaction energies calculated above, calculations that neglect polarization can recreate certain experimentally observed characteristics of the channel, for example, the K^+/Na^+ selectivity. However, calculations of polarization energy indicate that polarization plays a nontrivial role in the energetics of ion diffusion, with structural features of the channel influencing the binding energy. Notably, we observed a reduction in the magnitude of the polarization energy in the S2 binding site, this pattern being repeated for KirBac and KcsA with K^+ and Rb^+ ions, and in a less consistent way for Na^+. This effect, at least in part, appears to be due to the influence of a second ion polarizing the V76 residue, affecting the interaction energy of the ion near S2. This has potential implications for the modeling of these systems. While substantial progress toward understanding the mechanism of K^+ channels has been made through single-ion, single-binding site models of the selectivity filter, by modeling multiple ion positions and including polarization effects, it has been shown that the interplay between an ion and a binding site in the channel can be affected by interactions taking place in other sites in the channel. In order to derive a fully accurate picture of the behavior of an ion in one binding site, the behavior of ions

in the remainder of the channel should be considered. In addition, while many excellent studies of free energy differences in selection and permeation have been carried out using nonpolarizable classical force fields, the observation here of multi-ion polarization effects cannot be ignored. Whether the differences caused by polarization would translate into energetic or geometrical differences in a fully polarizable model of dynamics is a question for future research. However, our results support the consensus of opinion that polarizable models are of great importance in modeling ion channel systems.

Acknowledgment. C.D. thanks The Royal Society for a University Research Fellowship. This work was supported by grants from The Leverhulme Trust and the EPSRC. The Oxford Supercomputing Center and HECToR are acknowledged for providing computational resources.

Supporting Information Available: (1) Details of the RCC method for defining ion channel positions. (2) Lists of residues included in the polarized MM region of the calculations on KcsA and KirBac. (3) Figure S1. (4) Figure S2. (5) Figure S3. (6) Figure S4. (7) Figure S5. (8) List of residues included in the polarized MM region of the calculations. (9) Details of smoothing algorithm used for plotting energy data. This information is available free of charge via the Internet at http://pubs.acs.org/.

References

(1) Doyle, D. A.; Cabral, J. M.; Pfuetzner, R. A.; Kuo, A. L.; Gulbis, J. M.; Cohen, S. L.; Chait, B. T.; MacKinnon, R. The structure of the potassium channel: Molecular basis of K^+ conduction and selectivity. *Science* **1998**, *280* (5360), 69–77.

(2) Kuo, A. L.; Gulbis, J. M.; Antcliff, J. F.; Rahman, T.; Lowe, E. D.; Zimmer, J.; Cuthbertson, J.; Ashcroft, F. M.; Ezaki, T.; Doyle, D. A. Crystal structure of the potassium channel KirBac1.1 in the closed state. *Science* **2003**, *300* (5627), 1922–1926.

(3) MacKinnon, R.; Cohen, S. L.; Kuo, A. L.; Lee, A.; Chait, B. T. Structural conservation in prokaryotic and eukaryotic potassium channels. *Science* **1998**, *280* (5360), 106–109.

(4) Hille, B. *Ion channels of excitable membranes*, 3rd ed.; Sinauer Associates: Sunderland, MA, 2001; pp 1−814.

(5) LeMasurier, M.; Heginbotham, L.; Miller, C. KcsA: It's a potassium channel. *J. Gen. Physiol.* **2001**, *118* (3), 303–313.

(6) Zhou, Y. F.; Morais-Cabral, J. H.; Kaufman, A.; MacKinnon, R. Chemistry of ion coordination and hydration revealed by a K^+ channel-Fab complex at 2.0 angstrom resolution. *Nature* **2001**, *414* (6859), 43–48.

(7) Berneche, S.; Roux, B. Energetics of ion conduction through the K^+ channel. *Nature* **2001**, *414* (6859), 73–77.

(8) Leech, J.; Prins, J. F.; Hermans, J. SMD: Visual steering of molecular dynamics for protein design. *IEEE Comput. Sci. Eng.* **1996**, *3* (4), 38–45.

(9) Aqvist, J.; Luzhkov, V. Ion permeation mechanism of the potassium channel. *Nature* **2000**, *404* (6780), 881–884.

(10) Domene, C.; Klein, M. L.; Branduardi, D.; Gervasio, F. L.; Parrinello, M. Conformational changes and gating at the selectivity filter of potassium channels. *J. Am. Chem. Soc.* **2008**, *130* (29), 9474–9480 .

(11) (a) Allen, T. W.; Kuyucak, S.; Chung, S. H. Molecular dynamics study of the KcsA potassium channel. *Biophys. J.* **1999**, *77* (5), 2502–2516. (b) Kuyucak, S.; Andersen, O. S.; Chung, S. H. Models of permeation in ion channels. *Rep. Prog. Phys.* **2001**, *64* (11), 1427–1472. (c) Roux, B.; Berneche, S. On the potential functions used in molecular dynamics simulations of ion channels. *Biophys. J.* **2002**, *82* (3), 1681–1684.

(12) Bucher, D.; Raugei, S.; Guidoni, L.; Dal Peraro, M.; Rothlisberger, U.; Carloni, P.; Klein, M. L. Polarization effects and charge transfer in the KcsA potassium channel. *Biophys. Chem.* **2006**, *124* (3), 292–301.

(13) Ban, F. Q.; Kusalik, P.; Weaver, D. F. Density functional theory investigations on the chemical basis of the selectivity filter in the K^+ channel protein. *J. Am. Chem. Soc.* **2004**, *126* (14), 4711–4716.

(14) Kariev, A. M.; Znamenskiy, V. S.; Green, M. E. Quantum mechanical calculations of charge effects on gating the KcsA channel. *BBA Biomembr.* **2007**, *1768* (5), 1218–1229.

(15) (a) Kariev, A. M.; Green, M. E. Quantum mechanical calculations on selectivity in the KcsA channel: The role of the aqueous cavity. *J. Phys. Chem. B* **2008**, *112* (4), 1293–1298. (b) Kariev, A. M.; Green, M. E. Quantum calculations on water in the KcsA channel cavity with permeant and nonpermeant ions. *BBA Biomembr.* **2009**, *1788* (5), 1188–1192.

(16) (a) Varma, S.; Rempe, S. B. Tuning ion coordination architectures to enable selective partitioning. *Biophys. J.* **2007**, *93* (4), 1093–1099. (b) Thomas, M.; Jayatilaka, D.; Corry, B. The predominant role of coordination number in potassium channel selectivity. *Biophys. J.* **2007**, *93* (8), 2635–2643.

(17) (a) Huetz, P.; Boiteux, C.; Compoint, M.; Ramseyer, C.; Girardet, C. Incidence of partial charges on ion selectivity in potassium channels. *J. Chem. Phys.* **2006**, *124*, 4. (b) Compoint, M.; Ramseyer, C.; Huetz, P. Ab initio investigation of the atomic charges in the KcsA channel selectivity filter. *Chem. Phys. Lett.* **2004**, *397* (4−6), 510–515.

(18) Guidoni, L.; Carloni, P. Potassium permeation through the KcsA channel: a density functional study. *BBA* **2002**, *1563*, 1–6.

(19) Jorgensen, W. L. Special issue on polarization. *J. Chem. Theory Comput.* **2007**, *3* (6), 1877–1877.

(20) Gascon, J. A.; Leung, S. S. F.; Batista, E. R.; Batista, V. S. A self-consistent space-domain decomposition method for QM/MM computations of protein electrostatic potentials. *J. Chem. Theory Comput.* **2006**, *2* (1), 175–186.

(21) Svensson, M.; Humbel, S.; Froese, R. D. J.; Matsubara, T.; Sieber, S.; Morokuma, K. ONIOM: A multilayered integrated MO+MM method for geometry optimizations and single point energy predictions. A test for Diels-Alder reactions and Pt(P(t-Bu)(3))(2)+H-2 oxidative addition. *J. Phys. Chem.* **1996**, *100* (50), 19357–19363.

(22) (a) Luzhkov, V. B.; Aqvist, J. K+/Na+ selectivity of the KcsA potassium channel from microscopic free energy perturbation calculations. *BBA Protein Struct. Mol. Enzymol.* **2001**, *1548* (2), 194–202. (b) Noskov, S. Y.; Berneche, S.; Roux, B. Control of ion selectivity in potassium channels by electrostatic and dynamic properties of carbonyl ligands. *Nature* **2004**, *431* (7010), 830–834. (c) Bostick, D. L.; Brooks, C. L. Selectivity in K+ channels is due to topological control of the permeant

ion's coordinated state. *Proc. Natl. Acad. Sci. U.S.A.* **2007**, *104* (22), 9260–9265 .

(23) Harding, M. M. Metal-ligand geometry relevant to proteins and in proteins: sodium and potassium. *Acta Crystallogr., Sect. D* **2002**, *58*, 872–874.

(24) Varma, S.; Rempe, S. B. Coordination numbers of alkali metal ions in aqueous solutions. *Biophys. Chem.* **2006**, *124* (3), 192–9.

(25) Bucher, D.; Guidoni, L.; Carloni, P.; Rothlisberger, U. Coordination Numbers of K^+ and Na^+ Ions Inside the Selectivity Filter of the KcsA Potassium Channel: Insights from First Principles Molecular Dynamics. *Biophys. J.* **2010**, *98* (10), L47–L49.

(26) Bezanilla, F.; Armstrong, C. M. Negative conductance caused by entry of sodium and cesium ions into potassium channels of squid axons. *J. Gen. Physiol.* **1972**, *60* (5), 588–&.

(27) (a) Furini, S.; Beckstein, O.; Domene, C. Permeation of water through the KcsA K^+ channel. *Proteins* **2009**, *74* (2), 437–448. (b) Domene, C.; Sansom, M. S. P. Potassium channel, ions, and water: Simulation studies based on the high resolution X-ray structure of KcsA. *Biophys. J.* **2003**, *85* (5), 2787–2800.

(28) Lockless, S. W.; Zhou, M.; MacKinnon, R. Structural and thermodynamic properties of selective ion binding in a K+ channel. *Plos Biol.* **2007**, *5* (5), 1079–1088.

(29) Kraszewski, S.; Boiteux, C.; Langner, M.; Ramseyer, C. Insight into the origins of the barrier-less knock-on conduction in the KcsA channel: molecular dynamics simulations and ab initio calculations. *Phys. Chem. Chem. Phys.* **2007**, *9* (10), 1219–1225.

(30) Dudev, T.; Lim, C. Determinants of K+ vs Na+ Selectivity in Potassium Channels. *J. Am. Chem. Soc.* **2009**, *131* (23), 8092–8101.

(31) Illingworth, C. J.; Domene, C. Many-body effects and simulations of potassium channels. *Proc. R. Soc. London, Ser. A* **2009**, *465* (2106), 1701–1716.

(32) Zhou, Y.; Morais-Cabral, J. H.; Kaufman, A.; MacKinnon, R. Chemistry of ion coordination and hydration revealed by a K^+ channel-Fab complex at 2.0 Å resolution. *Nature* **2001**, *414*, 43–48.

(33) Kuo, A.; Gulbis, J. M.; Antcliff, J. F.; Rahman, T.; Lowe, E. D.; Jochen, Z.; Cuthbertson, J.; Ashcroft, F. M.; Ezaki, T.; Doyle, D. A. Crystal structure of the potassium channel KirBac1.1 in the closed state. *Science* **2003**, *300*, 1922–1926.

(34) Berneche, S.; Roux, B. The ionization state and the conformation of Glu-71 in the KcsA K^+ channel. *Biophys. J.* **2002**, *82* (2), 772–780.

(35) Humphrey, W.; Dalke, A.; Schulten, K. VMD: Visual molecular dynamics. *J. Mol. Graphics* **1996**, *14* (1), 33.

(36) (a) MacKerell, A. D.; Bashford, D.; Bellott, M.; Dunbrack, R. L.; Evanseck, J. D.; Field, M. J.; Fischer, S.; Gao, J.; Guo, H.; Ha, S.; Joseph-McCarthy, D.; Kuchnir, L.; Kuczera, K.; Lau, F. T. K.; Mattos, C.; Michnick, S.; Ngo, T.; Nguyen, D. T.; Prodhom, B.; Reiher, W. E.; Roux, B.; Schlenkrich, M.; Smith, J. C.; Stote, R.; Straub, J.; Watanabe, M.; Wiorkiewicz-Kuczera, J.; Yin, D.; Karplus, M. All-atom empirical potential for molecular modeling and dynamics studies of proteins. *J. Phys. Chem. B* **1998**, *102* (18), 3586–3616. (b) Brooks, B. R.; Bruccoleri, R. E.; Olafson, B. D.; States, D. J.; Swaminathan, S.; Karplus, M. CHARMM: A program for macromolecular energy, minimisation, and dynamics calculations. *J. Comput. Chem.* **1983**, *4*, 187–217.

(37) Jorgensen, W. L.; Chandresekhar, J.; Madura, J. D.; Impey, R. W.; Klein, M. L. Comparison of simple potential functions for simulating liquid water. *J. Chem. Phys.* **1983**, *79*, 926–935.

(38) Essmann, U.; Perera, L.; Berkowitz, M. L.; Darden, T.; Lee, H.; Pedersen, L. G. A smooth particle mesh Ewald method. *J. Chem. Phys.* **1995**, *103* (19), 8577–8593.

(39) Miyamoto, S.; Kollman, P. A. SETTLE - an analytical version of the Shake and Rattle algorithm for rigid water models. *J. Comput. Chem.* **1992**, *13* (8), 952–962.

(40) Tuckerman, M.; Berne, B. J.; Martyna, G. J. Reversible multiple time scale molecular-dynamics. *J. Chem. Phys.* **1992**, *97* (3), 1990–2001.

(41) (a) Martyna, G. J.; Tobias, D. J.; Klein, M. L. Constant pressure molecular-dynamics algorithms. *J. Chem. Phys.* **1994**, *101* (5), 4177–4189. (b) Feller, S. E.; Zhang, Y. H.; Pastor, R. W.; Brooks, B. R. Constant-pressure molecular dynamics simulation- the langevin piston method. *J. Chem. Phys.* **1995**, *103* (11), 4613–4621.

(42) (a) Phillips, J. C.; Braun, R.; Wang, W.; Gumbart, J.; Tajkhorshid, E.; Villa, E.; Chipot, C.; Skeel, R. D.; Kale, L.; Schulten, K. Scalable molecular dynamics with NAMD. *J. Comput. Chem.* **2005**, *26* (16), 1781–1802. (b) Kale, L.; Skeel, R.; Bhandarkar, M.; Brunner, R.; Gursoy, A.; Krawetz, N.; Philips, J.; Shinozaki, A.; Varadarajan, K.; Schuten, K. Molecular dynamics programs design - NAMD2: Greater Scalability for Parallel Molecular Dynamics. *J. Comp. Phys.* **1999**, *151*, 283–312.

(43) Morais-Cabral, J. H.; Zhou, Y. F.; MacKinnon, R. Energetic optimization of ion conduction rate by the K+ selectivity filter. *Nature* **2001**, *414* (6859), 37–42.

(44) (a) Allen, T. W.; Bliznyuk, A.; Rendell, A. P.; Kuyucak, S.; Chung, S. H. The potassium channel: Structure, selectivity and diffusion. *J. Chem. Phys.* **2000**, *112* (18), 8191–8204. (b) Guidoni, L.; Carloni, P. Potassium permeation through the KcsA channel: a density functional study. *BBA Biomembr.* **2002**, *1563* (1−2), 1–6. (c) Domene, C.; Vemparala, S.; Furini, S.; Sharp, K.; Klein, M. L. The role of conformation in ion permeation in a K+ channel. *J. Am. Chem. Soc.* **2008**, *130* (11), 3389–3398.

(45) Furini, S.; Domene, C. Atypical mechanism of conduction in potassium channels. *Proc. Natl. Acad. Sci. U.S.A.* **2009**, *106* (38), 16074–16077.

(46) Illingworth, C. J. R.; Gooding, S. R.; Winn, P. J.; Jones, G. A.; Ferenczy, G. G.; Reynolds, C. A. Classical polarization in hybrid QM/MM methods. *J. Phys. Chem. A* **2006**, *110* (20), 6487–6497.

(47) Illingworth, C. J. R.; Parkes, K. E.; Snell, C. R.; Marti, S.; Moliner, V.; Reynolds, C. A. The effect of MM polarization on the QM/MM transition state stabilization: application to chorismate mutase. *Mol. Phys.* **2008**, *106* (12−13), 1511–1515.

(48) Illingworth, C. J. R.; Morris, G. M.; Parkes, K. E. B.; Snell, C. R.; Reynolds, C. A. Assessing the Role of Polarization in Docking. *J. Phys. Chem. A* **2008**, *112* (47), 12157–12163.

(49) Frisch, M. J.; Trucks, G. W.; Schlegel, H. B.; Scuseria, G. E.; Robb, M. A.; Cheeseman, J. R.; Montgomery, J. A.; Vreven, J. T.; Kudin, K. N.; Burant, J. C.; Millam, J. M.; Iyengar, S. S.; Tomasi, J.; Barone, V.; Mennucci, B.; Cossi, M.; Scalmani, G.; Rega, N.; Petersson, G. A.; Nakatsuji, H.; Hada,

M.; Ehara, M.; Toyota, K.; Fukuda, R.; Hasegawa, J.; Ishida, M.; Nakajima, T.; Honda, Y.; Kitao, O.; Nakai, H.; Klene, M.; Li, X.; Knox, J. E.; Hratchian, H. P.; Cross, J. B.; Bakken, V.; Adamo, C.; Jaramillo, J.; Gomperts, R.; Stratmann, R. E.; Yazyev, O.; Austin, A. J.; Cammi, R.; Pomelli, C.; Ochterski, J. W.; Ayala, P. Y.; Morokuma, K.; Voth, G. A.; Salvador, P.; Dannenberg, J. J.; Zakrzewski, V. G.; Dapprich, S.; Daniels, A. D.; Strain, M. C.; Farkas, O.; Malick, D. J.; Rabuck, A. D.; Raghavachari, K.; Foresman, J. B.; Ortiz, J. V.; Cui, Q.; Baboul, A. G.; Clifford, S.; Cioslowski, J.; Stefanov, B. B.; Liu, G.; Liashenko, A.; Piskorz, P.; Komaromi, I.; Martin, R. L.; Fox, D. J.; Keith, T.; Al-Laham, M. A.; Peng, C. Y.; Nanayakkara, A.; Challacombe, M.; Gill, P. M W.; Johnson, B.; Chen, W.; Wong, M. W.; Gonzalez, C.; Pople, J. A. *Gaussian 03*; Gaussian Inc.: Wallingford, CT, 2009.

(50) Stone, A. J. *J. Chem. Theory Comput.* **2005**, *1*, 1128–1132.

(51) Ferenczy, G. G.; Reynolds, C. A. Modeling polarization through induced atomic charges. *J. Phys. Chem. A* **2001**, *105* (51), 11470–11479.

(52) Bliznyuk, A. A.; Rendell, A. P. Electronic effects in biomolecular simulations: Investigation of the KcsA potassium ion channel. *J. Phys. Chem. B* **2004**, *108* (36), 13866–13873.

(53) Marcus, Y. The thermodynamics of solvation of ions. 2 The enthalpy of hydration at 298.15 K. *J. Chem. Soc., Faraday Trans. 1* **1987**, *83*, 339–349.

(54) (a) Berneche, S.; Roux, B. Molecular dynamics of the KcsA K^+ channel in a bilayer membrane. *Biophys. J.* **2000**, *78* (6), 2900–2917. (b) Khalili-Araghi, F.; Tajkhorshid, E.; Schulten, K. Dynamics of K+ ion conduction through Kv1.2. *Biophys. J.* **2006**, *91* (6), L72−4. (c) Miloshevsky, G. V.; Jordan, P. C. Conformational changes in the selectivity filter of the open-state KcsA channel: An energy minimization study. *Biophys. J.* **2008**, *95* (7), 3239–3251. (d) Grottesi, A.; Domene, C.; Sansom, M. Permeation and gating in KirBac: Molecular dynamics simulations. *Biophys. J.* **2004**, *86* (1), 178A–178A.

CT100276C